The finite-element behaviour simulation of the rotary-type and frame-type solar sails on the geocentric orbits

I Gorbunova, R Khabibullin, S Chernyakin and O Starinova
Spacecraft department, Samara State Aerospace University, 151, Molodogvardeiskaya st., Samara 443086, Russia

E-mail: gorbunovairina88@gmail.com

Abstract. This paper discusses the research of functioning of different construction types for the spacecraft with a solar sail. Two types of the solar sail are considered, such as frame-type and rotary-type. The research is performed by means of application of the computer-assisted design system. The movement simulation of the spacecraft center mass and the forces acting on the solar sail is described. The finite element models of the two solar sail constructions are developed and compared.

1. Introduction
Nowadays the world leading space nations are actively developing missions focused on the near-Earth space investigation. A promising way of cost reduction for such missions is the use of advanced physical principles of space flight. One of those principles is the development of a solar sailing technology, which allows considerable saving in energy.

The greatest advantage of a solar sailing concept is that it allows the creation of propellant free systems, implying that they can accelerate indefinitely. The absence of propellant means a major saving of mass, together with the fact that there is no engine; the energy to mass ratio of the spacecraft can be very high. Both these factors together mean that the solar sail spacecraft is able to reach high velocities, which is crucial for deep interplanetary travel and especially interstellar travel [1].
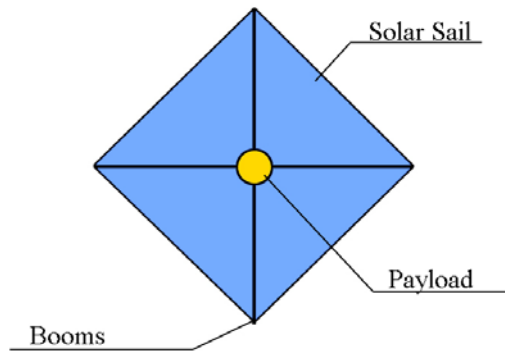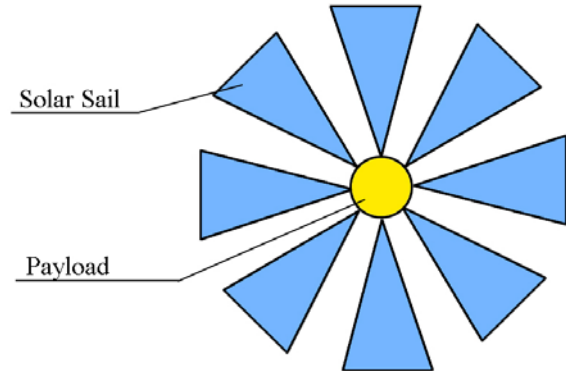
2. Solar sail configurations
Solar sails are a form of spacecraft propulsion, which accelerates by means of pressure of stellar radiation on large ultra-thin mirrors.

At present, all solar sails launched into space are carefully folded to fit in the upper stage of the launch vehicle, and deployed when the spacecraft is in space. The sails are generally made of a three-layered film. The layer which faces the Sun is made of highly reflective aluminum, which is fixed to the central layer of a plastic substrate. One commonly used substrate is Kapton. An emissive layer, often chromium, is fixed to the side of the sail directed away from the Sun. Its function is to dissipate the heat produced by the small amount of solar flux which is absorbed by the sail's aluminum front face.

The most reliable and effective solar sail configurations are a frame-type solar sail (Figure 1) and a rotary-type solar sail (Figure 2) [5].

Figure 1. Frame-type solar sail.

Figure 2. Rotary-type solar sail.

The frame construction of the solar sail is the most simple and reliable structure, that is based on a rigid truss or a frame foundation, to which the parts of the sail are attached. It is a heavy and strong design with a small windage (the ratio of the area of the solar sail to the mass of the spacecraft). The advantage of this construction is reliable sail fixing - they do not curl up and it is easy to control them.

The rotor construction is a more perspective and lightweight structure that provides deployment and support of the sail due to centrifugal forces of inertia. Sails of this type are designed as parts of various shapes attached to the central body of the spacecraft. For some rotating spacecraft small weights are attached to the ends of solar sail vanes or on ropes (which deploys the solar sail), thus increasing the force of inertia. This construction provides a lower mass compared to the frame, and therefore, higher windage.

3. Movement simulation of the centre mass of the spacecraft
The mathematical models and control laws obtained in [4] are used to model the maneuvers to achieve parabolic speed on orbits of different heights Starting circular orbits of different heights are used. Problems of the attitude control were not considered in this paper.
Traditional differential equations in a matrix-vector form are used to simulate the geocentric motion of the spacecraft:

$$\frac{d\mathbf{V}}{dt} = \mathbf{f} + \mathbf{a} \ , \ \mathbf{J}\frac{d\boldsymbol{\omega}}{dt} = \mathbf{M} \tag{1}$$

Here $\mathbf{V}$ is the velocity, $\mathbf{f}$ is the acceleration from gravity, aerodynamics and other disturbing forces, $\mathbf{a}(\lambda_1, \lambda_2)$ is the acceleration from the light pressure forces, $\mathbf{J}$ is the solar sail spacecraft inertia tensor, $\boldsymbol{\omega}$ is the angular velocity, $\mathbf{M}$ is the moment of the external forces applied to the spacecraft.

Sail angle setting (the angle between the normal to the plane of the sail and the direction of the sun) is determined by two control angles: $\lambda_1(t)$ - the angle between the projection of the thrust vector to the instantaneous velocity of the orbit and the radius vector of the gravitational center of the spacecraft, and $\lambda_2(t)$ - the angle between the thrust vector and the normal to the instantaneous plane of the spacecraft path. As the control laws of the solar sail spacecraft are used locally, optimal control laws of setting the sail angle are obtained in [2]. For the first of them, it is supposed that the spacecraft moves in the ecliptic plane and the normal to the plane of the sail also lies in plane ($\lambda_1(t){\equiv}0$), and angle $\lambda_1(t)$ is defined proceeding from maximizing of projection of the accelerate spacecraft on a transversal direction of the object-centred coordinate system. In this case,

$$\lambda_{1opt} = \frac{1}{2}\left[\arcsin\left(\frac{S'_x}{3\left(S'^2_x + S'^2_y\right)^{\frac{1}{2}}} \right) - \arctg\left(\frac{S'_x}{S'_y} \right) \right] \tag{2}$$

Here S'_x, S'_y, and S'_z are components of the vector of the direction to the Sun.

Let us suppose now that $\lambda_1=90°$, that is, a sail rotation axis is directed by the local radius vector. In this case,

$$\lambda_{2opt} = \frac{1}{2}\left[\arcsin\left(\frac{S'_z}{3\left(S'^2_x + S'^2_y\right)^{\frac{1}{2}}} \right) - \operatorname{arctg}\left(\frac{S'_z}{S'_y} \right) \right] \qquad (3)$$

This control is convenient to implement travel of the gravity-oriented sail (the spacecraft is a construction extending along axis OX'). Herewith the plane of the orbit must be located as near as possible to terminator ($S'_x = S'_y \approx 0$) [2].

For a vehicle having a solar sail, considered in this project, the mass should be 50 kg, and the area should amount to 200 m^2. Table 1 shows the results of the calculation of the maneuver to achieve parabolic speed for the solar sail spacecraft with these design characteristics for the control laws.

Table 1. Results of the calculation of the maneuver to achieve parabolic speed for control law 1 and control law 2

Control law	Orbital altitude (km)	Required angular velocity	
		(deg/day)	(rad/sec)
Locally optimal law (1)	6000	1135.3	$0.229 \cdot 10^{-3}$
	18000	410.4	$0.083 \cdot 10^{-3}$
	36000	178.85	$0.036 \cdot 10^{-3}$
Locally optimal law (2)	6000	2271.46	$0.459 \cdot 10^{-3}$
	18000	821.66	$0.166 \cdot 10^{-3}$
	36000	358.56	$0.072 \cdot 10^{-3}$

The data in Table 1 show that in order to allow maneuvering the spacecraft at a lower altitude, it is essential that the construction allows sail reversals at higher speeds.

The ability of the solar sail spacecraft to maneuver at low orbits provides additional advantages compared to the spacecraft that can exist and function only at high orbits. First of all, it saves propellant fuel to launch the spacecraft to the start orbit. If the spacecraft is designed to capture the earth's surface, the use of a lower orbit functioning extends the possibility of optics. If the spacecraft is designed for photographing of a part of the earth's surface, it will increase the accuracy of the light direction and the light output [3].

4. Forces acting on the solar sail

Let us introduce a coordinate system associated with the undeformed surface of the solar sail, as shown in Figure 3. Plane xOy coincides with the plane of the undeformed solar sail. The Oz-axis is pointed at the angular velocity of sail rotation ω_1 (the sail ensures deployment and maintaining of it in a deployed state). The Ox axis is directed at the angular velocity of programmed reversal of the sail with angular velocity ω_2 (provides program control of the sail).

Let us consider an elementary area at the surface of the sails, which is small enough to neglect the change of the forces and its curvature in moving over its surface. The position of the elementary area is determined by the position of its center $\mathbf{r}_S=\{x_S, y_S, z_S\}$, the position of its plane - by current normal $\mathbf{n}=\{n_x, n_y, n_z\}$, $|\bar{n}|=1$. This area is acted upon by light pressure forces and the force of interaction with the neighboring areas. In case of the rotary-type solar sail the centrifugal force of rotating is considered.
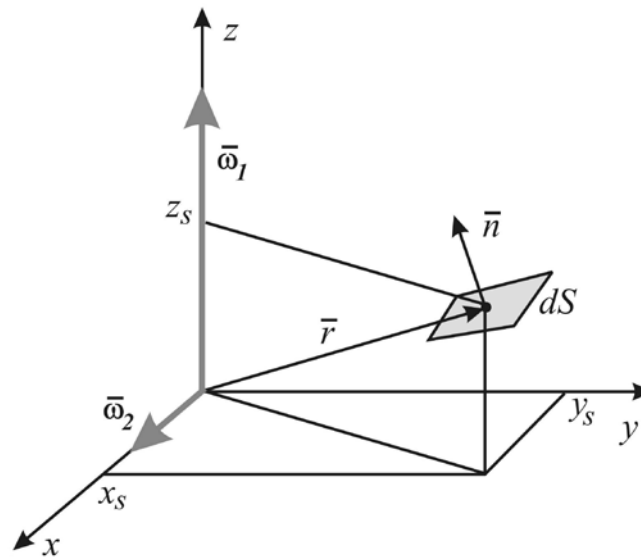
Figure 3. Scheme of the forces acting on the rotating element
of the solar sail.

The area is involved in the following movements:
- Motion of the spacecraft as a solid body-controlled movement is assumed to be given, it specifies the amount and direction of light pressure and the desired axis of rotation and the speed controlled reversal;
- Rotation of the solar sail spacecraft relative to the center of mass with angular velocity ω_1 providing the necessary rigidity of the sail surface, it determines the magnitude and direction of the centrifugal forces (in case of the rotary-type solar sail);
- Rotation of the spacecraft relative to the center of mass with angular velocity ω_2 that provides a thrust of a given direction.

If we assume that the Sun is located in the direction of Z, then the value of the light pressure force is defined by the following relationship [5]:

$$dF_C = P_a \cdot n_z^2 \cdot dS \tag{4}$$

The centrifugal force of inertia is determined by vector relation:

$$\mathbf{\Phi}_c = m\mathbf{W}_c = -dm \cdot \mathbf{\omega} \times \left(\mathbf{\omega} \times r\right) \tag{5}$$

where $\mathbf{\omega}=\mathbf{\omega}_1+\mathbf{\omega}_2=\{\omega_2, 0, \omega_1\}$ is the total angular velocity vector; $\mathbf{r}=\mathbf{r}_S=\{x_S, y_S, z_S\}$ is the radius vector of the area center relative to the origin of coordinates.
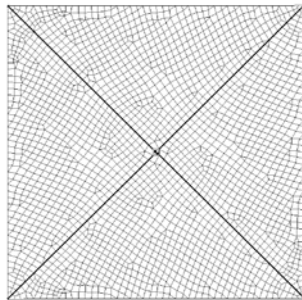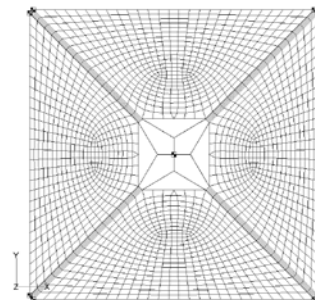
5. Finite Element Models
This paper describes the application of the method of the finite elements analysis applied to frame-type and rotary-type solar sails, with the help of finite elements simulation system.

The description of the frame-type and rotary-type solar sail spacecraft elements is given in Table 2. The finite element model of the frame-type and rotary-type solar sail of spacecrafts is shown in Figure 4 and Figure 5 respectively.

According to (4), (5) and Table 1 the forces influencing the solar sail are determined. Locally optimal law 2 is considered because it has greater angular velocity values. The list of force values acting at distances of 6000 km, 18000 km and 36000 km is presented in Table 3.

Table 2. Frame-type and rotary-type solar sail spacecraft elements description.

	Element of design	Type of element	Material	Properties
Common elements	Spacecraft	element of concentrated mass, absolutely rigid element RBE 2		Mass is 50 kg
	Solar sail	plate element	polyamide film Kapton	Young's Modulus is 2500 MPa thickness is $7.5 \cdot 10^{-3}$ mm
Frame-type only	Booms	beam element	carbon fiber	Young's Modulus is 67000 MPa thickness is 2 mm length is 10000 mm
Rotary-type only	Ropes	beam elements with significantly reduced rigidity	kevlar	thickness is 2 mm
	End weights	elements concentrated mass	carbon fiber	mass is 0.25 kg
	Coupling member between ropes	shell element flexural thick shell	polyamide film	Young's Modulus is 3200 MPa thickness is 2 mm

Figure 4. A finite element model of the frame-type solar sail.

Figure 5. A finite element model of the rotary-type solar sail.

Table 3. Force values acting on the solar sail for locally optimal law 2

Type of the solar sail	Orbital altitude (km)	Max forces of the rotation with ω_1 (N)	Max Sun pressure (N)	Max forces of rotation with $\omega2$ (N)
Frame-type	6000	$F_x=F_y=F_z=0$		$F_x=F_y=73.738 \cdot 10^{-6}$, $F_z=0$
	18000	$F_x=F_y=F_z=0$		$F_x=F_y=9.645 \cdot 10^{-6}$, $F_z=0$
	36000	$F_x=F_y=F_z=0$		$F_x=F_y=1.814 \cdot 10^{-6}$, $F_z=0$
Rotary-type	6000	$F_x=F_y=78.819 \cdot 10^{-3}$, $F_z=0$	$1.856 \cdot 10^{-6}$	$F_x=78.819 \cdot 10^{-3}$, $F_y=77.950 \cdot 10^{-3}$, $F_z=0$
	18000	$F_x=F_y=10,354 \cdot 10^{-3}$, $F_z=0$		$F_x=10,354 \cdot 10^{-3}$ $F_y=9.546 \cdot 10^{-3}$, $F_z=0$
	36000	$F_x=F_y=1,947 \cdot 10^{-3}$, $F_z=0$		$F_x=1.947 \cdot 10^{-3}$ $F_y=1.012 \cdot 10^{-3}$, $F_z=0$

6. Results And Discussion

According to Table 3 the finite element simulation is performed. The strength analysis of the frame-type and rotary-type solar sails at distances of 6000 km, 18000 km and 36000 km is provided. Strain, stress and deformation of the finite element models are calculated according to strain and stress by mean of the computer-assisted design system. The examples of the strength analysis of the frame-type and rotary-type solar sails are shown in Figure 6 and Figure 7 respectively.
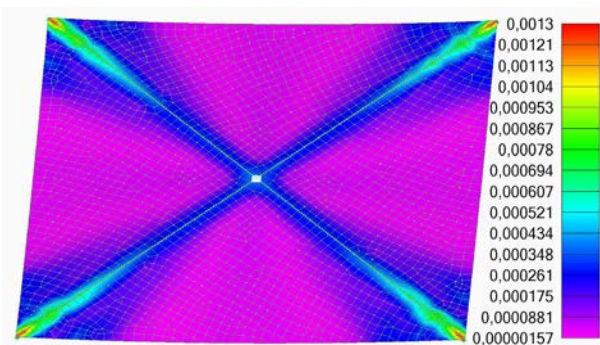

Figure 6. Stress distribution [MPa] on the solar sail surface of the frame-type solar sail.
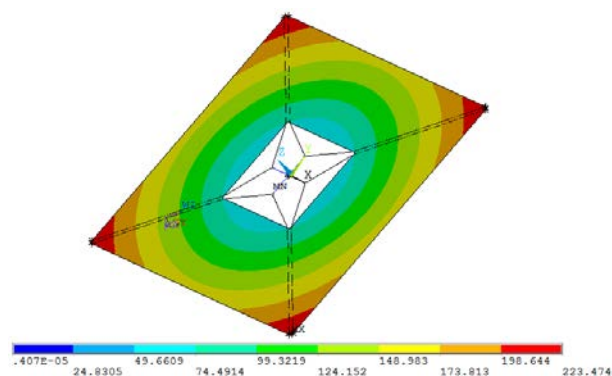
Figure 7. Stress distribution [Pa] of the rotary-type solar sail during deployment.

Having finished the nonlinear static analysis we have obtained the following results:
- the frame-type construction of the solar sail is stronger than the rotary-type construction;
- the frame-type solar sail is capable of flying 36000 km and 6000 km distance;
- the rotary type solar sail can operate with rotation speed of 450 deg/days, consequently the spacecraft should be in 36000 km orbit.

7. Conclusion

In this paper we investigated the interconnection of the behavior of the two different constructions of the solar sail spacecraft during maneuver on the geocentric orbit. The frame-type and rotary type solar sails were compared. The stability analysis of the constructions indicates the necessity of construction or changing the spacecraft control law. Modeling the behavior of the design allows coming to conclusion that the frame-type solar sail is stronger than the rotary-type solar sail, consequently the frame-type construction is capable of flying on lower orbits of 6000 km. In case of the rotary-type construction, the distance of 36000 km is more preferable.

Acknowledgment

References

[1]   Materials of http://interplanetarytravelandtheuniverse.webs.com
[2]   Ishkov S and Starinova O 2005 *Samara: The SSC RAS Publisher* **7(1)** 99–106
[3]   Salmin V, Starinova O and Ishkov S 2006 *Samara: The SSC RAS Publisher* 216
[4]   Starinova O 2007 *Samara: The SSC RAS Publisher* 196
[5]   Starinova O, Khabibullin R and Gorbunova I 2015 *Istanbul: IEEE Publisher* 643-648